Mid InfraRed Instrument (MIRI) Cooler Compressor Assembly Characterization

M. Petach, M. Michaelian, T. Nguyen, R. Colbert and J. Mullin

Northrop Grumman Aerospace Systems
Redondo Beach, CA 90278 USA

ABSTRACT

The Cooler Subsystem for the Mid InfraRed Instrument (MIRI) of the James Webb Space Telescope (JWST) utilizes a remotely mounted subassembly containing a compressor and gas precooler to provide pressurized and precooled gas to the Cold Head Assembly as the final cooling stage of the precooled Joule-Thomson cooler. The flight model subassembly, called the Cooler Compressor Assembly, has been built and has completed its in-process performance testing prior to delivery to acceptance testing. This paper describes the Cooler Compressor Assembly and summarizes its cryogenic refrigeration performance results.

INTRODUCTION

The Mid InfraRed Instrument Cooler Subsystem (MIRI Cooler) is a closed cycle helium Joule-Thomson (JT) cryocooler precooled by a three-stage pulse tube cryocooler. The basic architecture and design parameters of this cooler have been described previously [1,2,3,4,5,6,7]. The MIRI Cooler consists of four major subassemblies that are integrated into the spacecraft separately and then interconnected. These four subassemblies (Figure 1) are:

- The Cryocooler Electronics Assembly (CCEA)
- The Cryocooler Compressor Assembly (CCA)
- The Cryocooler Tower Assembly (CTA)
- The Cold Head Assembly (CHA)

This paper focuses on the Cryocooler Compressor Assembly (CCA), which is the cooler subassembly that compresses and precools the helium working fluid. The CCA (Figure 1) resides within the JWST observatory's spacecraft bus. The major assemblies of the CCA are the three-stage Pulse Tube Precooler, the PT Precooler Helium compressor, and a series of recuperators that provide the thermal isolation between the room temperature helium from the JT compressor and as well as between the precooler's three stages. In the first box at the left margin of Figure 1, "CCEA" stands for Cryocooler Control Electronics Assembly, "RSA" stands for Relay Switch Assembly, and "JT P, JT R, PT P, and PT R" stand for primary and redundant JT and PT cryocooler control electronics. In the highlighted box "CCA", "PT" indicates the various Pulse Tube cold heads, "P_{high}" and "P_{low}" indicate pressure transducers and "HX" stands for various heat exchangers between the precooler and the 1st, 2nd, and 3rd stage recuperators. The next box to the right, "CTA" stands for the Cooler

Cryocoolers 19, edited by S.D. Miller and R.G. Ross, Jr.

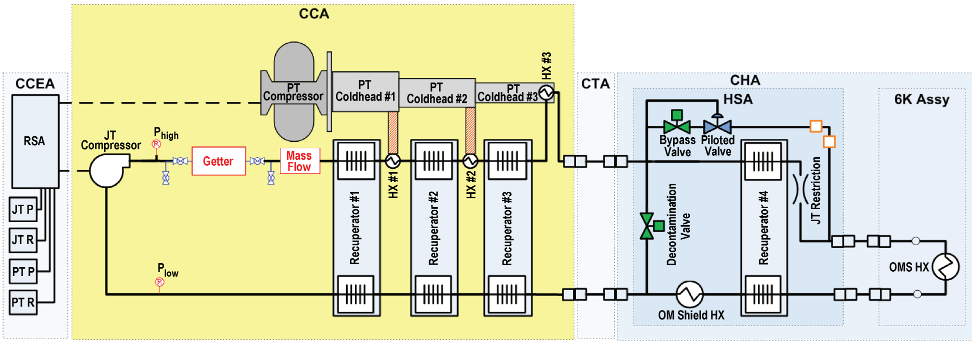

Figure 1. Functional block diagram of the entire MIRI Cryocooler system, highlighting the Cryocooler Compressor Assembly (CCA).

Tower Assembly. In the large box to the right, "CHA" stands for the remote Cold Head Assembly; it is divided into the "HSA" (Heat Sink Assembly) and the 6 K Assembly. Within the CHA, "OM_Shield HX" stands for the optical module shield heat exchanger, and "OMS HX" is the low temperature (6 K) heat exchanger that cools the MIRI optical bench and its focal plane modules.

The two major subassemblies of the CCA (JT compressor and PT precooler) were tested independently before being integrated together on the CCA's thermal interface plate. The JT compressor contains a single stage which provides a nominal helium gas flow of 25mg/s at approximately 12 bar on the high side and 4 bar on the low side. The PT precooler combines the PT compressor and the three-stage pulse tube cold heads that provide cooling at the nominally 150K, 50K and 18K helium precooling stages. The three recuperators associated with the PT precooler provide thermal isolation between the aforementioned precooling stages.

COOLER SUBSYSTEM PERFORMANCE TESTING RESULTS

JT Compressor

The Flight Model and Flight Spare JT Compressors were tested as stand-alone components for performance and exported forces. The performance of each compressor was tested by pumping helium through a load valve with a pneumatic impedance that was varied to mimic the range of flow impedances experienced with the flight system. The performance of each compressor is shown in Table 1. The summary includes key pertinent performance characteristics, including reject temperature, frequency, pressures, mass flows and compressor powers. The two flight compressors met subsystem requirements.

The JT compressor exported force was measured on a 6-axis force dynamometer, with data shown in Figure 2. The JT compressor was operated at acceptance level power with a representative pneumatic restriction used in place of the nominal system JT restriction.

Table 1. JT Compressor Performance Summary

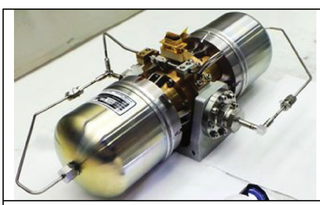	Date/ Time	T_{reject}, K	Freq, Hz	P_{hi}, bar abs.	P_{lo}, bar abs.	Mass flow, mg/s	Comp. Power, W
Flight Model CCA1 ZF610	10-27-14, 13:07	305	90.06	11.53	4.10	24.5	67.6
Flight Spare CCA2 ZF607	7-24-15, 18:51	305	90.06	11.48	4.01	24.4	78.6

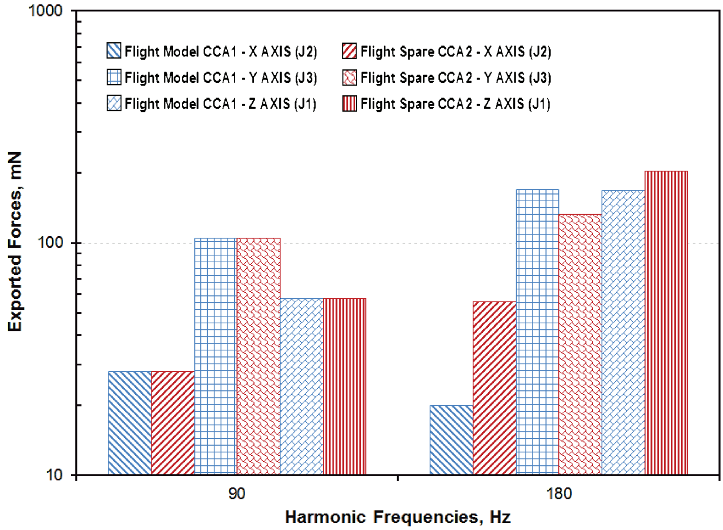

Figure 2. Exported force results at the fundamental drive frequency (90 Hz) and 2nd harmonic (180 Hz) for the JT Flight Model and Flight Spare compressors.

The amplitudes of the various exported forces are plotted for each compressor axis in units of mN peak, with Flight Model and Flight Spare results adjacent to one another for each axis. The key result from this figure is that the exported forces in the JT compressor drive axis were on the order of 50 mN and less for both the drive frequency and 2nd harmonic, whereas the off-axis exported forces were all less than 200 mN.

Launch vibration testing of the JT compressor was not conducted at the component level and was instead deferred to CCA level vibe tests. The basis for this was that the JT compressor is the same as the TRL9 NGAS High Efficiency Cryocooler (HEC) compressor (Figure 3), with over a dozen units in Flight Operation, and the only major change from these units was the reed valve design that was validated with valve-module-level vibration tests [2]. Vibration testing of the JT compressor at CCA assembly level was successful and will be described in a future paper.

PT Precooler

The PT Precooler design was derived from the NGAS 10K Pulse Tube Cooler [2,7]. The precooler contains a three-stage pulse tube with stages operating at 150K, 50K and 18K. The PT

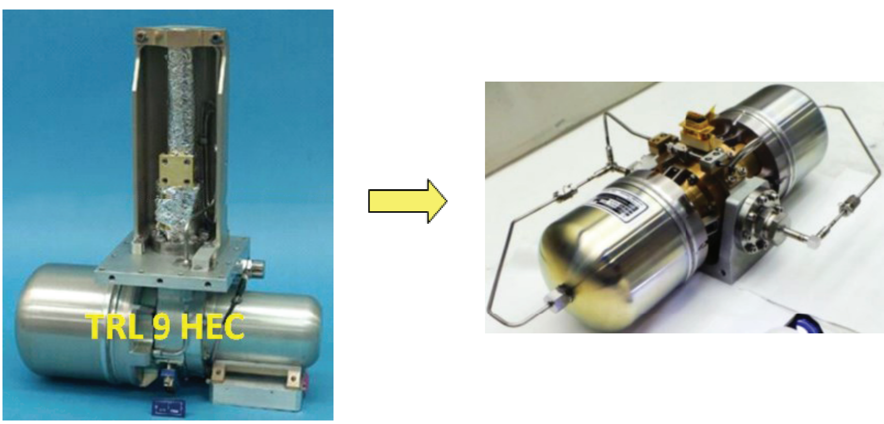

Figure 3. TRL 9 HEC Heritage of the MIRI JT compressor

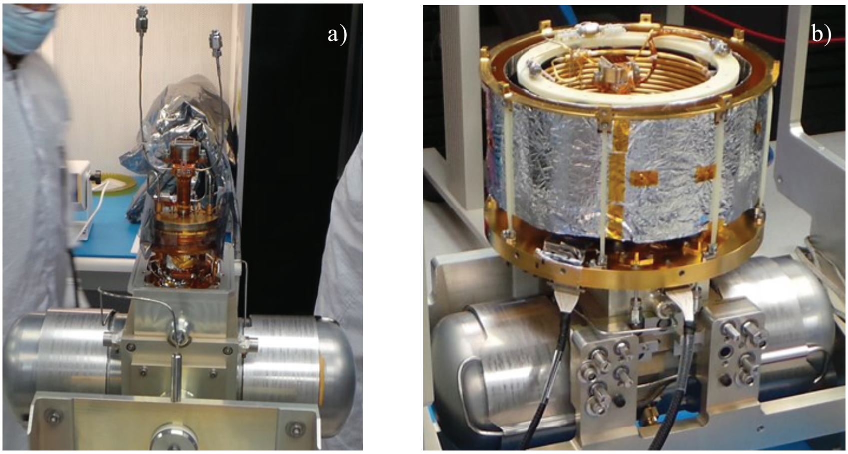

Figure 4. PT Precooler configurations: a) Cooler-Only (without recuperators and flight shields) (left figure) and b) Cooler plus flight recuperators and flight shields (right figure)

cooler was first tested at the Cooler-Only level (Part# 460026), which contains only the compressor and the pulse tube cold heads, as shown in Figure 4a. It was tested again at a higher level of assembly (Part# 460120) – containing the cooler along with flight recuperators and the two flight thermal shields that its upper stages cool, as shown in Figure 4b. The second test was completed in order to verify minimal impact to the system performance as a result of the added flight hardware. In the case of the Cooler plus flight recuperators/thermal shields, the refrigeration performance was initially measured *without helium gas flow* to confirm the minimal impact of the parasitic thermal loads of the recuperative and flight shield hardware. Later, using the same cooler configuration, precooler performance was measured *with helium gas flow* through the JT circuit using a representative pneumatic restriction to reproduce approximate flight mass flow rates and pressures, with electrical heat added to measure lift. Figure 5 shows pinch-point-condition [6] load lines for the Flight Model and Flight Spare PT precoolers for the third stage at the Cooler-only level (Part# 460026). The

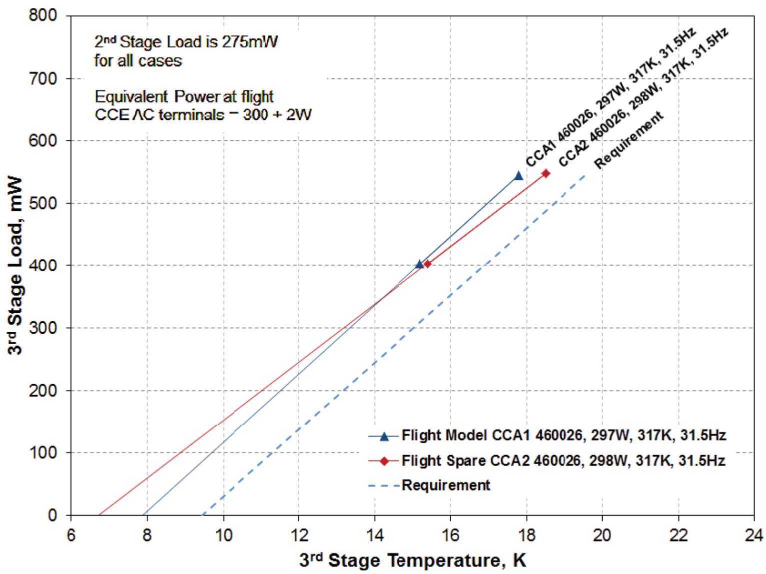

Figure 5. Three-stage Pulse Tube Precooler Refrigeration performance at Cooler-Only level (460026).

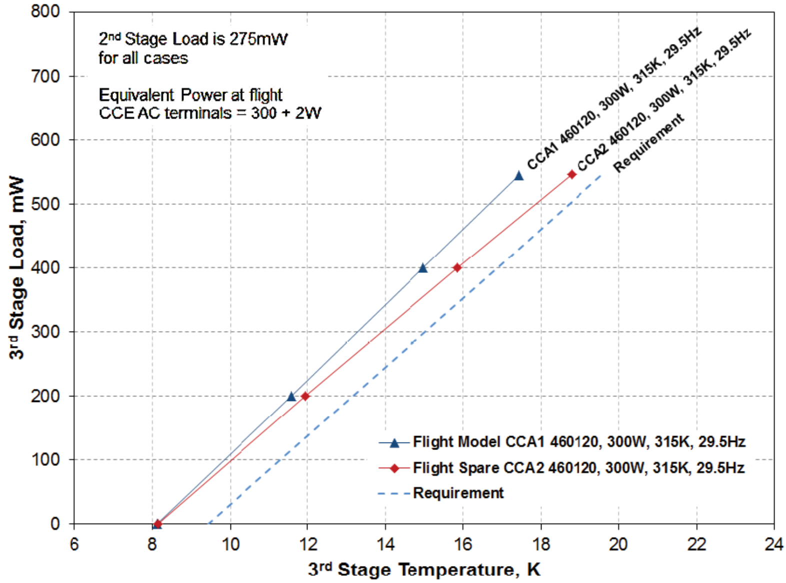

Figure 6. Three-stage Pulse Tube Precooler Refrigeration performance at Cooler plus flight recuperators/ thermal shields level (460120).

environmental condition for all data shown has a constant 2nd Stage load of 275 mW applied at approximately 50 K to simulate the expected flight loads on the 2nd Stage shield. The power applied to the PT compressor in all cases was an equivalent compressor power at Flight CCEA AC terminals of 300 W. Figure 6 shows the pinch-point condition load line performance at the next higher level of assembly with cooler plus flight recuperators/thermal shields (Part# 460120). Figure 7 shows the combined plot of pinch point load line data from the two aforementioned assembly levels. The Precooler refrigeration performance data at both assembly levels were better than the requirement and were consistent with previous end-to-end cooler tests using the DM precooler and FM Cold Head Assembly [6].

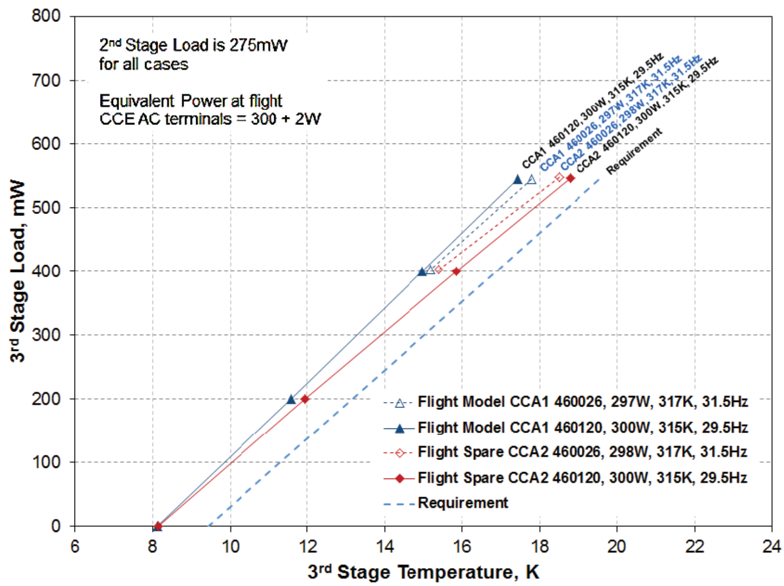

Figure 7. Three-stage Pulse Tube Precooler Refrigeration performance at both assembly levels.

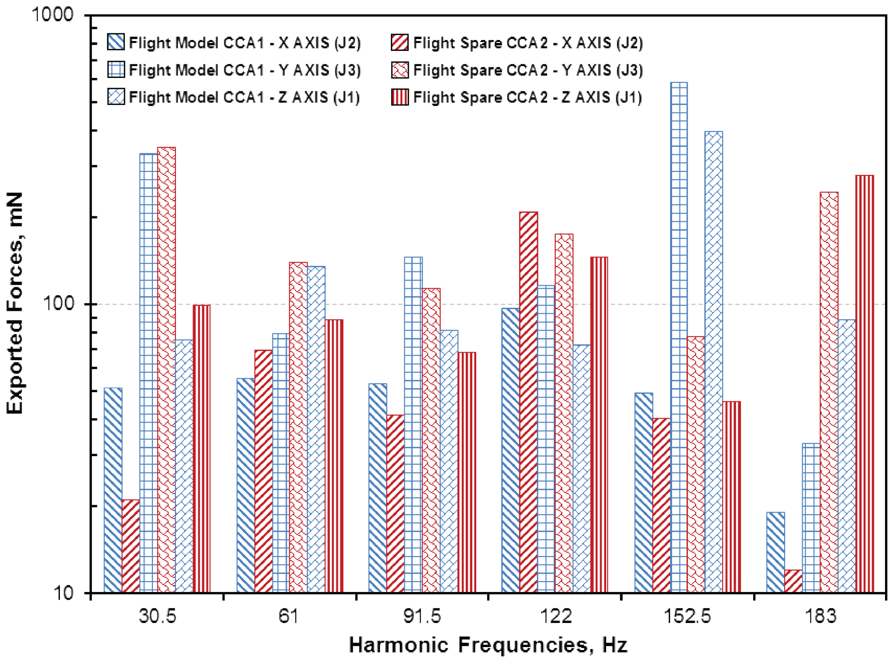

Figure 8. Exported force results for PT Flight Model and Flight Spare compressors.

The three-stage PT Precooler was also tested to quantify its exported forces. The three-stage PT Precoolers were tested on the same 6-axis force dynamometer as the JT compressors and were tested at the cooler plus flight recuperator/thermal shields level (Part# 460120), with the recuperative heat exchangers and flight thermal shields attached. Like the refrigeration performance testing, the external loads on the precooler were kept constant at 275mW at 50K and greater than 500mW at 18K. The results from the three-stage Precoolers are shown in Figure 8. All six axes of the Flight Model and Flight Spare assemblies were measured, with X, Y and Z forces reported here. The abscissa of Figure 8 shows a nominal drive frequency of 30.5, with the 2nd through 5th harmonics shown with increasing frequency. The 1st and 2nd bars in each frequency correspond to the drive, or X-axis exported forces, the 3rd and 4th bars delineating the Y-axis exported forces and the 5th and 6th bars corresponding to the Z-axis exported forces, as measured on the 6-axis dynamometer. The key result from this figure is that the exported forces due to the PT compressor drive axis were less than 100 mN throughout the drive frequency through the first six harmonics, whereas the off-axis exported forces were all less than 600 mN, with many around 100 mN or less.

The three-stage pulse-tube Precooler was additionally exposed to random vibration environmental testing. The Flight Model and Flight Spare were tested at acceptance levels of approximately 0.1 g2/Hz. All post-vibe checkouts indicated nominal results. The post-vibe refrigeration performance was later measured at the CCA level and confirmed the operational integrity of the CCA. CCA testing results will be reported in a future paper.

The PT and JT compressors are the only shock sensitive components in the CCA, thus they needed to be flight qualified for resistance to shock. As previously mentioned, the HEC Compressor design used in the JT Compressor for the JT loop had been qualified for this shock environment on several previous flight programs, so additional flight qualification for that compressor was not needed.

In contrast, the HCC Compressor used for the three-stage PT precooler needed to be qualified for the shock levels of the MIRI program. This was accomplished via a ringing plate test of an NGAS-owned compressor that is essentially identical to the MIRI compressor. Figure 9 shows the shock level profile established for the MIRI cooler mounting environment and the results of the

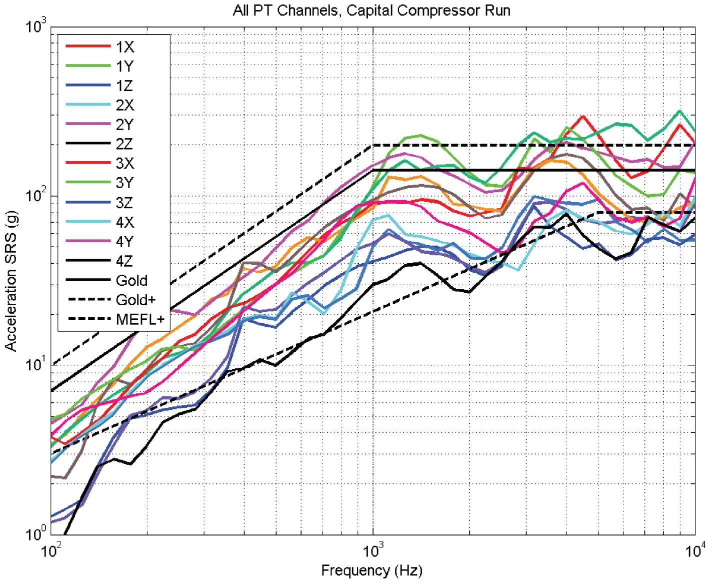

Figure 9. Shock acceleration profile established for the MIRI PT cooler mounting environment compared with measured levels achieved during the PT-cooler shock qualification test.

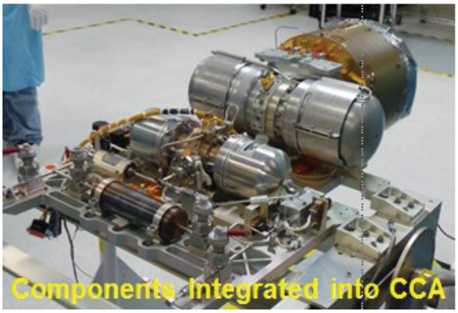

Figure 10. MIRI Cryocooler Compressor Assembly integrated and ready for shipping.

actual test profiles achieved in the test of the NGAS-owned compressor. Post-test measurements confirmed that the compressor was not affected by the shock exposure.

CONCLUSION

The MIRI Cooler Compressor Assembly components have all been characterized by in-process tests before integration onto the CCA. The Flight Model and Flight Spare CCA subassemblies have been successfully delivered to Acceptance testing at the CCA level (Figure 10).

The Component level characterization data acquired as a result of the MIRI Cooler CCA Sub Assembly test campaign are applicable to future space missions which might use a different configuration of these components.

ACKNOWLEDGMENT

This work was performed for the Jet Propulsion Laboratory, California Institute of Technology, sponsored by the United States Government under a Prime Contract between the California Institute of Technology and NASA.

REFERENCES

1. D. Durand, J. Raab, R. Colbert, M. Michaelian, T. Nguyen, M. Petach, and E. Tward, "NGST Advanced Cryocooler Technology Development Program (ACTDP) Cooler System," *Advances in Cryogenic Engineering: Transactions of the Cryogenic Engineering Conference – CEC*, vol. 51, edited by J. G. Weisend II (2006), pp. 615-622.
2. D. Durand, R. Colbert, C. Jaco M. Michaelian, T. Nguyen, M. Petach, and E. Tward, "NGST Advanced Cryocooler Technology Development Program (ACTDP) Cooler System," *Cryocoolers 14,* ICC Press, Boulder, Colorado (2007), pp. 21-29.
3. D. Durand, R. Colbert, C. Jaco M. Michaelian, T. Nguyen, M. Petach, and J. Raab, "Mid InfraRed Instrument (MIRI) Cooler Subsystem Prototype Demonstration," *Advances in Cryogenic Engineering: Transactions of the Cryogenic Engineering Conference – CEC*, vol. 53, edited by J. G. Weisend II (2008), pp. 807-814.
4. D. Durand, D. Adachi, D. Harvey C. Jaco, M. Michaelian, T. Nguyen, M. Petach, and J. Raab, "Mid InfraRed Instrument (MIRI) Cooler Subsystem Design," *Cryocoolers 15,* ICC Press, Boulder, Colorado (2009), pp. 7-12.
5. M. Petach, M. Michaelian "MIRI Cooler System Design Update," *Cryocoolers 16*, ICC Press, Boulder, Colorado (2011), pp. 9-12.
6. M. Petach, M. Michaelian "Mid InfraRed Instrument (MIRI) Cooler Cold Head Assembly Acceptance Testing and Characterization," *Cryocoolers 18*, ICC Press, Boulder, Colorado (2014), pp. 11-17.
7. T. Nguyen, R. Colbert, D. Durand, C. Jaco M. Michaelian, and E. Tward, "10K Pulse Tube Cooler," *Cryocoolers 14,* ICC Press, Boulder, Colorado (2007), pp. 27-32.